Food Research International 157 (2022) 111227

Contents lists available at ScienceDirect

Food Research International

journal homepage: www.elsevier.com/locate/foodres

Black corn (*Zea mays* L.) soluble extract showed anti-inflammatory effects and improved the intestinal barrier integrity *in vivo* (*Gallus gallus*)

Thaisa Agrizzi Verediano [a], Hércia Stampini Duarte Martino [b], Nikolai Kolba [a], Yimin Fu [a], Maria Cristina Dias Paes [c], Elad Tako [a,*]

[a] Department of Food Science, Cornell University, Stocking Hall, Ithaca, NY 14853, USA
[b] Nutrition and Health Department, Universidade Federal de Viçosa, Viçosa 36571-000, Minas Gerais, Brazil
[c] Empresa Brasileira de Pesquisa e Agropecuária (EMBRAPA), Sete Lagoas 35701-970, MG, Brazil

ARTICLE INFO

Keywords:
Polyphenols
Anthocyanin
Intestinal morphology
Intestinal barrier
Goblet cell
Cyanidin
Intra-amniotic

ABSTRACT

Black corn (*Zea mays L.*) is a pigmented type of this cereal whose color of the kernels is attributed to the presence of the anthocyanins. In this study, we assessed the black corn soluble extract (BCSE) effects on the intestinal functionality, morphology, and microbiota composition using an *in vivo* model (*Gallus gallus*) by an intra-amniotic administration. The eggs were divided into four groups (n = 6–10): (1) No Injection; (2) 18 MΩ H_2O/cm; (3) 5% (5 mg/mL) BCSE; (4) 15% (15 mg/mL) BCSE. The BCSE showed anti-inflammatory effects by down regulating the gene expression of tumor necrosis factor-alpha (TNF-α), interleukin 6 (IL6), and the transcriptional nuclear factor kappa beta (NF-κB). Further, the BCSE increased the relative abundance of *E. coli* and *Clostridium*. 5% and 15% BCSE increased the hepatic glycogen and upregulated the gene expression of sodium-glucose transport protein (SGLT1). In the morphology, 5% and 15% BCSE increased the goblet cell (GC) number on the crypt, the GC size on the villi, Paneth cell number on the crypt, and the acid GC. Further, the BCSE strengthened the epithelial physical barrier through upregulating the intestinal biomarkers AMP- activated protein kinase (AMPK) and caudal-related homeobox transcriptional factor 2 (CDX2). The overall result suggests that the BCSE promotes intestinal anti-inflammatory effects as well as enhances the intestinal barrier function.

1. Introduction

Black corn (*Zea mays L.*) is a colored cereal grain with claimed health benefits due to its bioactive components, mainly anthocyanins (Yang & Zhai, 2010; Van Hung, 2014; Ranilla et al., 2017; Zhu, 2018). The anthocyanins content in colored maize can vary widely due factors such as maize genetics, growing locations, part of the plant, extraction method, identification, and quantification (Harakotr et al., 2014). In this context, studies have shown a range of anthocyanin content from 23 to 252 mg anthocyanin/kg in a survey with 398 genotypes of pigment corn (Paulsmeyer et al., 2017) and from 12.8 to 93 mg cyanidin-3-glucoside (C3G) equivalents/g in 20 purple corn genotypes (Zhang et al., 2019). Anthocyanins, a subclass of flavonoids, are bioactive water-soluble pigmentss accountable for a wide range of blue, purple, violet, and red in fruits, flowers, and vegetables. In plants, anthocyanins are found mainly as a glycoside, with the basic structure as an anthocyanidin core attached to a sugar and organic acids (Sui et al., 2019). Beneficial health effects have been established to anthocyanins in preventing or improving risk factors associated with obesity (Azzini et al., 2017; Jamar et al., 2017; Lee et al., 2017), diabetes mellitus (Guo et al., 2007; Jurgoński et al., 2013; Różańska & Regulska-Ilow, 2018), metabolic syndrome (Bhaswant et al., 2017), mucositis (Tong et al., 2017), and colorectal cancer (Fernández et al., 2018; de Sousa Moraes et al., 2019). In this sense, anthocyanin acts as an antioxidant component by scavenging reactive oxygen species and as an anti-inflammatory through downregulating specific transcription factors such as the nuclear factor-kappa B (NF- κB), thus decreasing the expression of pro-inflammatory cytokines as tumor necrosis factor-alpha (TNF-α), interleukin (IL) 6 and IL1β (Vendrame & Klimis-Zacas, 2015; Bendokas et al., 2020).

Regarding the anthocyanin metabolism, briefly, a small proportion of the intaked anthocyanin is absorbed intact through the upper gastrointestinal wall by active transporters (Faria et al., 2014). Thus, most anthocyanin reaches the colon, where they are metabolized into their metabolites by bacteria from the intestinal microbiota. *Bifidobacterium* spp. and *Lactobacillus* spp. have the enzyme β-glucosidase, which is necessary to metabolize the anthocyanin into sugar and

* Corresponding author.
E-mail address: et79@cornell.edu (E. Tako).

https://doi.org/10.1016/j.foodres.2022.111227
Received 14 February 2022; Received in revised form 4 April 2022; Accepted 5 April 2022
Available online 6 April 2022

phenolic acids. Therefore, their metabolites modulate the growth of specific beneficial bacteria in the gut microbiota (Faria et al., 2014; Hribar & Ulrih, 2014). A systematic review recently showed that anthocyanin supplementation in animal studies could modulate the intestinal microbiota by increasing *Lactobacillus* spp. and *Bifidobacterium* spp. and improving short-chain fatty acids (SCFA) production. Further, anthocyanin can improve the epithelial barrier through a higher tight junction expression and mucus production by increasing the goblet cell differentiation due its fermentative action (Verediano et al., 2021). Besides, it is suggested that phenolic components founded in a purple potate extract might improve the barrier function through activating the AMP- activated protein kinase (AMPK) pathway, which activates the caudal-related homeobox transcriptional factor 2 (CDX2). By this, the upregulation of CDX2 controls the intestinal epithelial differentiation, and might regulate the tight junctions expression (Sun et al., 2018). However, this pathway has only been verified in an *in vitro* model (Sun et al., 2018). Futher, anthocyanin mix showed potential to improve occludin expression and Mucin 2 (MUC2) level, which might be used as biomarkers to tight junction functionality and intestinal barrier integrity (Cremonini et al., 2019).

To assess the prebiotic effects of nutrients on intestinal functionality and gut microbiota, the intra-amniotic administration in *Gallus gallus* model has been used as a valid approach (Hartono et al., 2015; Hou & Tako, 2018; da Silva et al., 2019; Dias et al., 2019; Wang et al., 2019; Gomes et al., 2021). The *Gallus gallus* is an established *in vivo* model to investigate the intestinal microbiome population due to its homology of gene sequence in the phylum levels with human (Yegani & Korver, 2008; Hou-Tako, 2018). The intra-amniotic administration of soluble extracts of beans, wheat, chia and yacon had demonstrated prebiotic effects by improving intestinal morphology, microbial composition and functionality (da Silva et al., 2019; Wang et al., 2019; Martino et al., 2020). Also, the administration of resveratrol and pterostilbene promoted beneficial morphological changes and improved the gut microbiota composition and function (Gomes et al., 2021). In this context, although some mechanisms have been proposed to explain how anthocyanin improves the intestinal barrier *in vivo*, there are no studies investigating the effects of black corn soluble extract, source of bioactive components, mainly anthocyanin, in the intestinal development.

Thus, we hypothesized that the black corn soluble extract as a source of anthocyanin could modulate the abundance of beneficial gut bacteria improving the intestinal physical barrier by upregulating the gene expression of proteins in the pathway of tight junction development. Therefore, showing improvement of the morphologic structure and brush border enzymes functionality. To explore this hypothesis, we designed an *in vivo* study investigating the effects of the intra-amniotic administration of black corn soluble extract (BCSE) on the intestinal morphology, functionality, and microbiota composition *in vivo* (*Gallus gallus)*.

2. Materials and methods

2.1. Sample preparation

The black corn (TO002) was provided by the Brazilian Agriculture Research Corporation (EMBRAPA). The TO002 black-color maize genotype is an access of the Maize Germplasm Bank of the Embrapa Maize and Sorghum. The material was produced in the 2018/2019 harvest season at "Embrapa Milho e Sorgo" experimental farm, Sete Lagoas, Minas Gerais, Brazil. The samples were stored in a plastic bag, kept at 4 ^{0}C, and protected from light until processing. The black corn flour was prepared using a knife mill grinder with a 1.0 mm stainless steel sieve (Willy, Solab®), which was stored at 4 ^{0}C.

2.2. Soluble extract from black corn

Soluble components extraction was performed as described (Tako et al., 2014). Black corn samples were dissolved in distilled water (50 g/L) (60 ^{0}C, 60 min) and centrifuged at 1200 *g* rpm (4 ^{0}C) for 25 min, and then the supernatant was collected. Then, the supernatant was dialyzed (MWCO 12–14 kDa) (48) against distilled water. The dialysate was collected and lyophilized to yield a fine off-white powder.

2.3. Phytate, dietary fiber, iron and zinc analysis in black corn flour and black corn extract

Dietary phytic acid (phytase)/total phosphorus was measured as phosphorus release by phytase and alkaline phosphatase, according to the manufacturers' instructions ($n = 5$) (K-PHYT 12/12; Megazyme International, Bray, Ireland). Total phytate concentrations were calculated with Mega-Calc™ by subtracting free phosphate concentrations in the extracts from the total amount of phosphorous that is exclusively released after enzymatic digestion. Total dietary fiber (soluble and insoluble fiber) was determined by the gravimetric-enzymatic method (AOAC International, 2012) using the enzymatic hydrolysis for a heat-resistant amylase, protease and amyloglucosidase (Total dietary fiber assay kit, Sigma®, San Luis, Missouri, EUA). The total dietary fiber content was determined by the sum between the soluble and insoluble fractions. For the determination of iron and zinc, briefly, black corn flour (0.5 g) and black corn extract (0.2 g) were pre-digested with 3.0 mL of a 60:40 (*v/v*) HNO_3 mixture in a Pyrex glass tube and left overnight to destroy organic matter. The analyses were carried out using an inductively coupled plasma atomic spectrometer (ICP-AES) (Thermo iCAP 6500 series, Thermo Scientific, Cambridge, UK). Yttrium from High Purity Standards (10 M67-1) was used as an internal standard to ensure batch-to-batch accuracy and correct matrix inference during digestion (da Silva et al., 2019; Dias et al., 2019).

2.4. Polyphenols analysis

2.4.1. Polyphenol extraction

The sample of black corn flour were extracted with 5.0 mL of methanol: formic acid 10% (*v/v*) solution, using sonication 40 KHz (USC 1400, Unique, Indaiatuba, SP) for 15 min. Then, the samples were centrifuged at 112 *g* for 10 min and the supernatant collected. This step was repeated 3 times. The supernatant was concentrated in rotary evaporator and 2 mL of deionized water was added. A total of 20 μL were removed and filtered to injection.

2.4.2. Chromatography profile and analysis of anthocyanins

The analysis was carried out using a liquid chromatography coupled to diode array detection and electrospray ionization tandem mass spectrometry (LC-DAD-ESI-MS/MS). The HPLC model was Varian 250 (Varian Inc., Lake Forest, CA) coupled with diode array detector (DAD) and mass spectrometer 500-MS IT (Varian Inc., Lake Forest, CA). The column was Symmetry C18 (3 μm, 250 × 2 mm) (Varian Inc., Lake Forest, CA). The flow rate was 0.4 mL/min and oven temperature of 30 ^{0}C. The mobile phase consisted of a combination of A (0.1% formic acid in water) and B (0.1% formic acid in acetonitrile). The gradient was varied linearly from 10 to 26% B (*v/v*) in 40 min, to 65% B at 70 min, and finally to 100% B at 71 min and held at 100% B at 75 min. The DAD was set up at 270 to 512 nm to monitor the UV/Vis absorption and the UV/Vis spectra were recorded from 190 to 650 nm. Mass spectra were acquired simultaneously using electrospray ionization in the positive and negative ionization (PI and NI) modes in voltage 80 V fragmentation for a mass range of 100–1000 amu. A drying gas pressure of 35 psi, nebulizer pressure of 40 psi, a drying gas temperature of 370 ^{0}C, capillary voltage of 3500 V for PI and 3500 V for NI, in addition to field voltages of 600 V spraying were used. The LC system was directly coupled to the MSD with 50% splitting.

Table 1
The sequence of experimental primers was used in this study.

Analyte	Forward Primers (5'-3')	Reverse Primers (5'-3')	Base Pairs Length	GI Identifier
BBM Functionality				
AP	CGTCAGCCAGTTTGACTATGTA	CTCTCAAAGAAGCTGAGGATGG	138	45,382,360
SI	CCAGCAATGCCAGCATATTG	CGGTTTCTCCTTACCACTTCTT	95	2,246,388
SGLT1	GCATCCTTACTCTGTGGTACTG	TATCCGCACATCACACATCC	106	8,346,783
Inflammatory Response				
IL1	TCATCCATCCCAAGTTCATTCA	GACACACTTCTCTGCCATCTT	105	395,872
TNF-α	GACAGCCTATGCCAACAAGTA	TTACAGGAAGGGCAACTCATC	109	53,854,909
NF-κB	CACAGCTGGAGGGAAGTAAAT	TTGAGTAAGGAAGTGAGGTTGAG	100	2,130,627
IL6	ACCTCATCCTCCGAGACTTTA	GCACTGAAACTCCTGGTCTT	105	302,315,692
Intestinal Barrier				
MUC2	CCTGCTGCAAGGAAGTAGAA	GGAAGATCAGAGTGGTGCATAG	272	423,101
OCLN	GTCTGTGGGTTCCTCATCGT	GTTCTTCACCCACTCCTCCA	124	396,026
AMPK	CTCCACTTCCAGAAGGTTACTT	GCAGTAGCTATCGTTCATCCTATC	140	427,185
CDX2	ACCAGGACGAAGGACAAATAC	CTTTCCTCCGGATGGTGATATAG	103	374,205
Glucose Metabolism				
G6PC*	GTCTGTCTGTCCCGCATTT	CATGGTAGATGGAGTGGATGTG	115	100,857,298
PCK1*	GCGATGGCTCAGAAGAAGAA	CTTGCTACGTCTCTTGGGTTAG	124	396,458
PKF*	AAGATGAAGACGACGGTGAAG	CCGTGTAGAGGTTGTAGATGAAG	94	374,064
18 s rRNA	GCAAGACGAACTAAAGCGAAAG	TCGGAACTACGACGGTATCT	100	7,262,899

AP: amino peptidase; SI: sucrose isomaltase; SGLT1: sodium-glucose transport protein 1; IL1: interleukin 1; TNF-α: tumor necrosis factor-alpha; NF-κB: nuclear factor kappa beta; IL6: interleukin 6; MUC2: mucin 2; OCLN: occludin; CDX2: caudal-related homeobox transcriptional factor 2; AMPK: AMP-activated protein kinase; G6PC: glucose-6 phosphatase; PCK1: phosphoenolpyruvate carboxykinase; PKF: phosphofructokinase 1. 18S rRNA: 18S ribosomal subunit. *Liver analyses.

2.5. In vivo experiment

Cornish cross-fertile broiler eggs (n = 40) were obtained from a commercial hatchery (Moyer's Chicks, Quakertown, PA, USA). The eggs were incubated under ideal conditions (37 ± 2 ^{0}C and 89.6 ± 2% humidity) at the Cornell University Animal Science poultry farm incubator. All animal protocols were approved by the Cornell University IACUC (protocol code: 2020–0077).

2.5.1. Intra-amniotic administration

The black corn soluble extract in powder form were diluted in 18 MΩ/cm H_2O to determine the concentrations necessary to maintain an osmolarity value (Osm) of < 320 OSM to ensure that the viable embryos would not be dehydrated upon injection of the solutions. The intra-amniotic administration followed the methodology previously described (Gomes et al., 2021; Martino et al., 2020). At the 17 days of embryonic development, eggs with viable embryos (n = 34) were randomly allocated into four groups with a similar weight frequency distribution using randomization software. All treatment groups were assigned eggs of similar weight frequency distribution. The experimental groups were assigned as follows: (1) non-injected (n = 10); (2) 18 MΩ/cm H_2O (n = 10); (3) 5% (5 mg/mL) black corn soluble extract (n = 8); (4) 15% (15 mg/mL) black corn soluble extract (n = 6). A total of 1 mL of solution per egg was injected into the amniotic fluid (identified by candling) with a 21-gauge needle. After the administration, the injection holes were sealed with cellophane tape, and the eggs were placed in hatching baskets to reduce possible allocation bias. On day 21, the hatchlings euthanized immediately after hatching by CO_2 exposure and the proximal small intestine (duodenum), blood, pectoral muscle, cecum, and liver were collected. The cecum and liver were weighed prior to freezing (liquid nitrogen). The following ratios were calculated: cecum weight/body weight and liver weight/body weight.

2.6. Blood analysis and hemoglobin measurements

The blood sample was collected using micro-hematocrit heparin-coated capillarity tuber (Fisher Scientific, Waltham, MA, USA) immediately after hatch but before euthanization. The hemoglobin (Hb) concentration was assessed spectrophotometric using the Quanti-Chrom™ Hb Assay (DIHB-250, BioAssay Systems, Hayward, CA, USA) and according to manufacturers' instructions.

2.7. Glycogen analysis

The pectoral muscle and liver (20 mg) were collected for glycogen analysis. The tissue samples were homogenized in 8% perchloric acid, and glycogen content was determined as described by (Dreiling et al., 1987) with modifications. All samples were read at a wavelength of 450 nm in an ELISA (Epoch, Biotek Instruments®, USA) plate reader and the amount of glycogen was obtained by a standard curve. The amount of glycogen present in the pectoral sample was determined by multiplying the weight of the tissue by the amount of glycogen per 1 g of wet tissue.

2.8. Extraction of the total RNA from the duodenum and liver tissue samples

The RNA was extracted from 30 mg of the proximal duodenum (as the main site of digestion and absorption) or liver (n = 5 animals/group) according to the manufacture's protocol (RNeasy Mini Kit, Qiagen Inc., Valencia, CA, USA) (Dias et al.; 2019; Martino et al., 2020; Gomes et al., 2021; Agarwal et al., 2022). All steps were carried out under RNase-free conditions. The total RNA was eluted in 50 μL of RNase-free water and RNA was quantified by absorbance at 260/280 and the integrity of the 18S ribosomal RNAs was verified by 1.5% agarose gel electrophoresis, followed by ethidium bromide staining. DNA contamination was removed using TURBO DNase treatment and removal kit from AMBION (Austin, TX, USA).

2.9. Real-time polymerase chain reaction (RT-PCR) and prime design

To obtain the cDNA, a total of 20 μL reverse transcriptase (RT) reaction was completed in a BioRad C1000 touch thermocycler using the Improm-II Reverse Transcriptase Kit (Catalog #A1250; Promega, Madison, WI, USA). The concentration of cDNA obtained was determined by

measuring the absorbance at 260 nm and 280 nm using an extinction coefficient of 33 (for single-stranded DNA). Genomic DNA contamination was assessed by a real-time RT-PCR assay for the reference genes samples (Dias et al., 2019). The sequences and the description of the primers used (Table 1) in the real-time qPCR was designed based on gene sequences from Genbank database, using Real-Time Primer Design Tool software (IDT DNA, Coralvilla, IA, USA) (Carboni et al., 2020; Dias et al., 2019; Martino et al., 2020). The specificity of the primers was tested by performing a BLAST search against the genomic National Center for Biotechnology Information (NCBI) database. The *Gallus gallus* primer 18S rRNA was designed as a reference gene. Results obtained from the qPCR system were used to normalize those obtained from the specific systems as described below.

2.10. Real-time qPCR design

Procedures were performed as previously described (da Silva et al., 2019; Martino et al., 2020; Gomes et al., 2021). cDNA was used for each 10 μL reaction containing 2 × BioRad SSO Advanced Universal SYBR Green Supermix (Hercules, CA, USA) Table 1 shows the primers used in this study. A "no template" control of nuclease-free water was included to eliminate DNA contamination in the PCR mix. For each reaction (duplicates), 8 μL of the master mix and 2 μL cDNA were pipetted into a 96-well plate, and for the standard curve, seven points were evaluated in duplicate. The double-stranded DNA was amplified in the Bio-Rad CFX96 Touch (Hercules, CA, USA) using the PCR conditions: initial denaturing at 95 ^{0}C for 30 s, 40 cycles of denaturing at 95 ^{0}C for 15 s, various annealing temperatures according to Integrated DNA Technologies (IDT) for 30 s and elongating at 60 ^{0}C for 30 s.The gene expression data were obtained as Cp values based on the "second derivative maximum" (automated method) as computed by Bio-Rad CFX Maestro 1.1 (Version 4.1.2433.1219, Hercules, CA, USA). The assays were quantified by including a standard curve in the real-time qPCR analysis, and a standard curve with four points was prepared by a 1:10 dilution (duplicates). The software produced a Cp vs. log 10 concentrations graph, and the efficiencies were calculated as 10 (1/slope). The specificity of the amplified real-time RT-PCR products was verified by melting curve analysis (60–95 ^{0}C) after 40 cycles, resulting in several different specific products with specific melting temperatures.

2.11. Collection of microbial samples and intestinal contents DNA extraction

The cecum was sterilely removed and treated as described previously (Hou et al., 2017). Briefly, the cecum contents were placed into a sterile 50 mL tube containing 9 mL of sterile PBS and homogenized by vortexing with glass beads (3 mm diameter) for 3 min. Debris was removed by centrifugation (700 *g* for 1 min), and the supernatant was collected and centrifuged at 12,000 *g* for 5 min. The pellet was washed twice with PBS and stored at −20 ^{0}C until DNA extraction. For DNA purification, the pellet was re-suspended in 50 mM EDTA and treated with lysozyme (Sigma Aldrich CO., St. Louis, MO, USA; final concentration of 10 mg/mL) for 45 min at 37 ^{0}C. The bacterial genomic DNA was isolated using a Wizard Genomic DNA purification kit (Promega Corp., Madison, WI, USA).

2.12. Primers design and PCR amplification of bacterial 16S rDNA

Primers for *Lactobacillus*, *Bifidobacterium*, *Clostridium* and *Escherichia coli* were used (Tako et al., 2008). The universal primers were designed with the invariant region in the 16S rRNA of bacteria and were used as internal standards. The proportions of each bacterial groups are presented. The PCR products were separated by 2% agarose gel, stained with ethidium bromide, and quantified by Quantity One 1-D analysis software (Bio-Ra, Hercules, CA, USA) (Dias et al., 2019). The relative abundance of each examined bacterium was evaluated as previously described (Tako et al., 2014; Dias et al., 2019). All products were expressed relative to the content of the universal 16 s rRNA primer product and proportions of each examined bacterial product.

Table 2
Chemical composition of black corn flour and black corn soluble extract.

	Black corn flour	Black corn soluble extract
Total dietary fiber (g/100 g)	13.25 ± 0.28^{a}	6.33 ± 0.04^{b}
Soluble dietary fiber (g/100 g)	0.31 ± 0.25^{a}	2.04 ± 0.42^{a}
Insoluble dietary fiber (g/100 g)	12.92 ± 0.03^{a}	4.29 ± 0.46^{b}
Iron (μg/g)	21.30 ± 0.29^{b}	154.12 ± 1.40^{a}
Zinc (μg/g)	26.18 ± 0.38^{b}	47.00 ± 1.49^{a}
Phytate (g/100 g)	0.705 ± 0.01^{b}	1.40 ± 0.14^{a}
Phytic acid: iron ratio	13.62 ± 0.26^{a}	7.72 ± 0.82^{b}

Values are means ± SED. Treatment groups not indicated by the same letter are different ($p < 0.05$) by t-Test.

2.13. Morphological examination of duodenal tissue

Intestinal morphology was performed as previously described (da Silva et al., 2019; Martino et al., 2020). The duodenum samples were fixed in fresh 4% (*v/v*) buffered formaldehyde, dehydrated, cleared and embedded in paraffin. Numerous sections were cut with a thickness of 5 μm and placed on glass slides. The sections were deparaffinized in xylene and rehydrated in a graded alcohol series. After, the slides were stained with Alcian Blue/Periodic acid-Schiff and examined by light microscopy. The following morphometric measurements were evaluated: villus height (μM), villus width (μM), depth of crypts (μM), goblet cell number and goblet cell diameter (μM) in the crypt and villi. Four segments for each biological sample with five biological samples per treatment group were performed with a light microscope using EPIX XCAN software (Standard version, Olympus, Waltham, MA, USA). For the Alcian Blue and Periodic acid-Schiff stain, the segments were only counted for the type of goblet cells (acid, neutral or mixed) in the villi epithelium, goblet cell within crypts and the mucus layer analysis. The goblet cells were enumerated at 10 villi/sample, and the means were calculated for statistical analysis. A representative duodenal histological cross-section image indicates the morphometric measurements from each experimental group.

2.14. Statistical analysis

Values were expressed as means ± standard error deviation (SED) from 6 to 10 biological samples per treatment group, except for intestinal morphology parameters analyses which used five biological samples. Experimental treatments for the intra-amniotic administration procedure were arranged in a completely randomized design. Effects of treatments were analyzed using a one-way Analysis of Variance (ANOVA). For significant "*p*-value," the post hoc Duncan test was used to compare test groups with the significant level at $p < 0.05$. The Kolmogorov-Smirnov normality test evaluated values for normal distribution and variance homogeneity. The statistical analyses were performed using the statistical software IBM SPSS Statistics®, version 20.

3. Results

3.1. Concentration of dietary fiber, iron, zinc, phytic acid, and phytate: Iron molar ration in black corn flour and black corn soluble extract

The concentration of iron, zinc and phytate was higher ($p < 0.05$) in the black corn soluble extract (BCSE) compared to the black corn flour. On the other hand, the content of total dietary fiber, insoluble dietary fiber, and phytic acid: iron ratio was lower in the BCSE relative to black corn flour. There was no difference in the concentration of soluble dietary fiber between the samples (Table 2). Related to the anthocyanin profile, cyanidin-3-glucoside was present in higher concentration (30.4

Table 3
Quantification of identified anthocyanin (mg/100 g), retention time and λ_{max} in black corn flour.

Anthocyanin	Amount (mg/100 g)	Retention time (min)	λ_{max}(nm)
Cyanidin-3-glucoside	30.40	20.66	515.28
Cyanidin-3-(6"-malonylglucoside)	17.60	29.69	517.28
Peonidin-3-glucoside	9.30	25.34	516.27
Peonidin-3-(6"malonylglucoside)	6.80	34.24	517.28
Pelargonidin-3-(6"malonylglucoside)	2.90	32.90	505.26
(epi)catechin-cyanidin-3,5-diglucoside	2.50	13.07	528.28
Pelargonidin-3-glucoside	2.40	23.75	501.28

Table 4
Effect of black corn soluble extract on body weight, cecum weight and cecum: bodyweight ratio.

	No Injection	H_2O Injection	5% BCSE	15% BCSE
Body weight (g)	40.060 ± 4.064[a]	47.490 ± 1.205[a]	45.150 ± 1.03[a]	42.730 ± 2.093[a]
Cecum weight (g)	0.420 ± 0.064[a]	0.470 ± 0.030[a]	0.450 ± 0.062[a]	0.425 ± 0.025[a]
Cecum:BW ratio	0.015 ± 0.005[a]	0.010 ± 0.001[a]	0.010 ± 0.001[a]	0.010 ± 0.001[a]
Hemoglobin (g/dL)	13.475 ± 1.314[a]	9.823 ± 0.772[a]	13.913 ± 3.835[a]	10.768 ± 1.784[a]

Values are means ± SED, $n = 6$–10/group. BW: body weight; BCSE: black corn soluble extract.
[a] Treatment groups indicated by the same letter are similar ($p > 0.05$) by *post-hoc* Ducan test.

mg/100 g) in the black corn flour (Table 3).

3.2. Effect of black corn soluble extract on biometric parameters

The body weight (BW), cecum weight and cecum: BW ratio was similar in the black corn soluble extract (5 and 15%) groups compared to the controls No Injection and H_2O Injection. In addition, all experimental groups showed similar levels of hemoglobin ($p > 0.05$) (Table 4).

3.3. Effect of black corn soluble extract on bacterial population in cecum contents

Regarding the bacterial population in cecum contents, the 5% BCSE showed lower ($p < 0.05$) abundance of *Bifidobacterium* compared to both controls groups (No Injection and H_2O Injection). The 15% BCSE showed similar abundance to the H_2O Injection group. The 5% BCSE and 15% BCSE groups showed similar abundance of *Lactobacillus* ($p > 0.05$) and lower abundance ($p < 0.05$) compared to the control groups (No Injection and H_2O Injection). Further, the 5% and 15% BCSE groups had an enriched abundance of *E. coli* ($p < 0.05$) compared to the H_2O Injection group. The abundance of *Clostridium* was higher ($p < 0.05$) in the 5% BCSE compared to the 15% BCSE, however, in both treatments of BCSE (5 and 15%), its abundance was similar to the H_2O Injection group (Fig. 1).

3.4. Effect of black corn soluble extract on gene expression of intestinal barrier proteins and brush border membrane functional proteins

Related to the intestinal barrier proteins, the gene expression of occludin (OCLN) was similar in all treatment groups. The intra-amniotic administration of 5% BCSE and 15% BCSE upregulated ($p < 0.05$) the gene expression of CDX2 compared to the No Injection and H_2O Injection groups. In the same way, the gene expression of AMPK was upregulated ($p < 0.05$) in the 5% BCSE compared to the H_2O Injection group. However, the 15% BCSE had similar levels compared to both control groups (No Injection and H_2O Injection). The gene expression of MUC2 was downregulated ($p < 0.05$) in the 5% BCSE and 15% BCSE compared to the control groups (No Injection and H_2O Injection) (Fig. 2A).

In addition, the intra-amniotic administration of 5% BCSE and 15% BCSE upregulated ($p < 0.05$) the gene expression of sodium-glucose transport protein (SGLT1) compared to the H_2O Injection control group. The gene expression of (sucrose isomaltase) SI was similar ($p > 0.05$) among all treatment groups, and (amino peptidase) AP was downregulated in the 5% BCSE and 15% BCSE groups compared to the H_2O Injection (Fig. 2A).

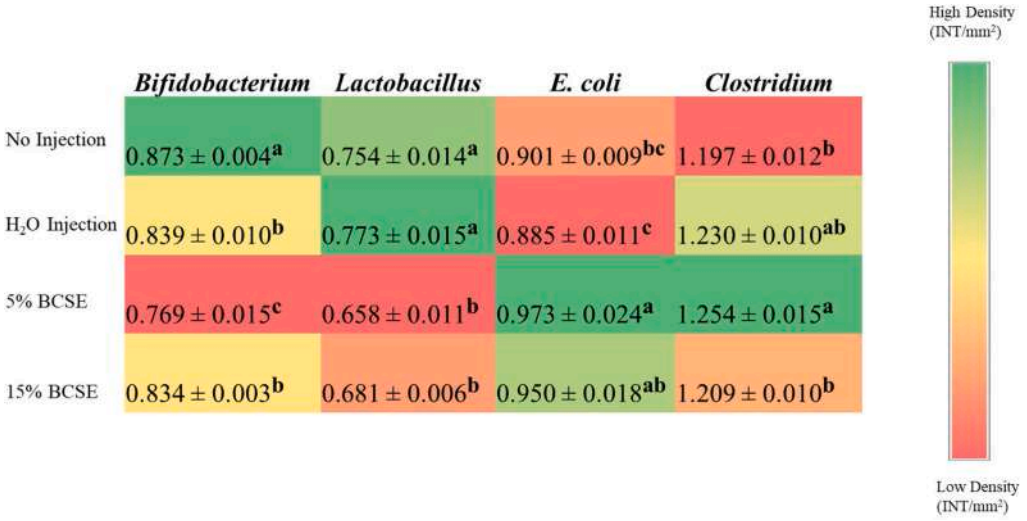

Fig. 1. Effect of intra-amniotic administration of black corn soluble extract on genera- and species-level bacterial population (AU) from cecal content measured on the day of hatch. BCSE: black corn soluble extract. Values are means ± SEM, $n = 5$/group. [a-c] Per bacterial category, treatment groups not indicated by the same letter are different ($p < 0.05$) by *post hoc* Duncan test.

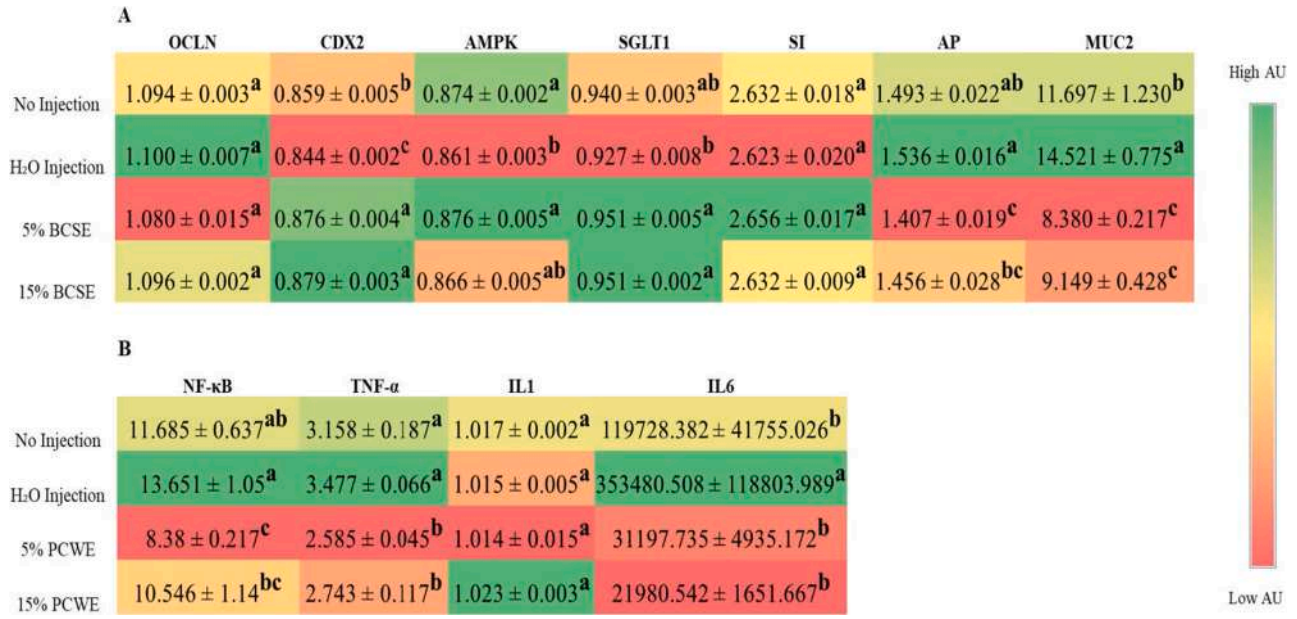

Fig. 2. Effect of black corn soluble extract on intestinal gene expression. Values are means ± SEM, $n = 5$/group. [a-c] Treatment groups not indicated by the same letter are different ($p < 0.05$) by *post hoc* Duncan test. BCSE: black corn soluble extract; OCLN: occludin; CDX2: caudal-type homeobox 2; AMPK: Adenosine Monophosphate (AMP)-activated protein kinase; SGLT1: sodium-glucose transport protein 1; SI: sucrose isomaltase; AP: amino peptidase; MUC2: mucin 2; NF-κB: nuclear factor kappa beta; TNF-α: tumor necrosis factor-alpha; IL1: interleukin 1; IL6: interleukin 6.

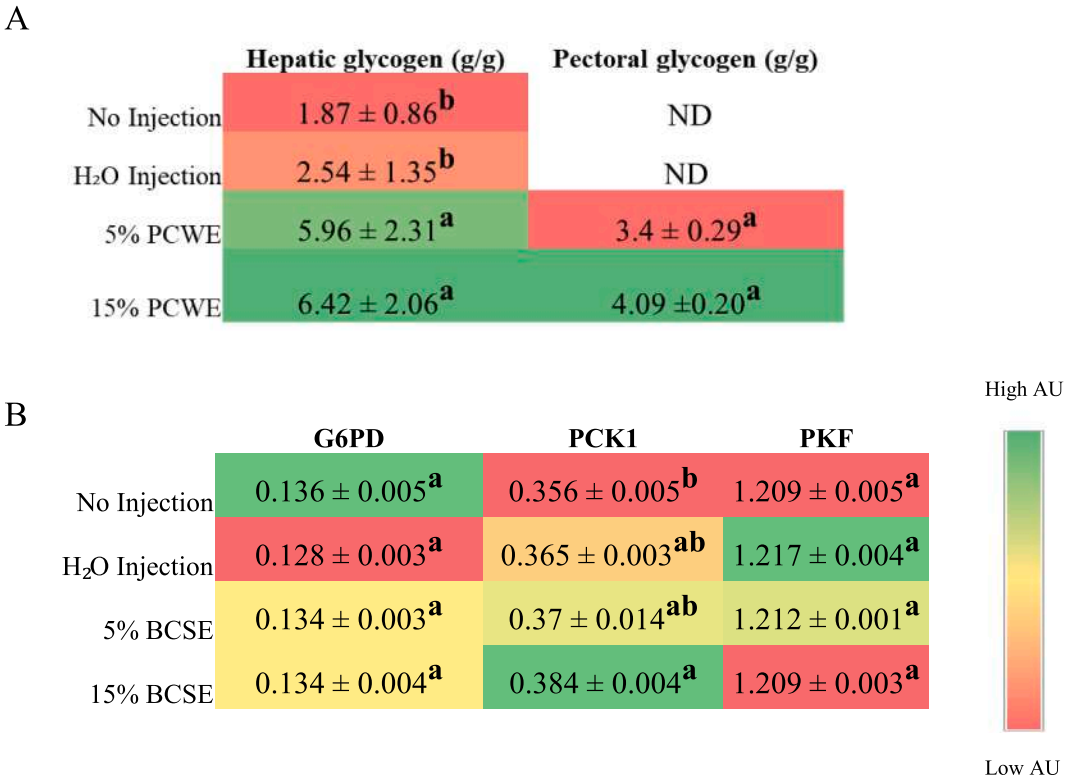

Fig. 3. Effect of black corn soluble extract (A) on hepatic gene expression and (B) on hepatic and pectoral glycogen concentration. Values are means ± SEM, $n = 5$/group. [a-c] Treatment groups not indicated by the same letter are different ($p < 0.05$) by *post hoc* Duncan test. BCSE: black corn soluble extract; ND: not detectable; G6PC: glucose-6 phosphatase; PCK1: phosphoenolpyruvate carboxykinase; PKF: phosphofructokinase.

3.5. Effect of black corn soluble extract on gene expression of inflammatory biomarkers

The intra-amniotic administration of black corn soluble extract improved inflammatory biomarkers (Fig. 2B). The gene expression of the transcription factor NF-κB was downregulated ($p < 0.05$) in the 5% BCSE group compared to both control groups (No Injection and H_2O Injection), and in the 15% BCSE was downregulated compared to the H_2O Injection group. Further, the 5% and 15% BCSE groups downregulated ($p < 0.05$) the gene expression of TNF-α compared to the

Table 5
Effect of black corn soluble extract on the duodenum.

Treatment group	Villi Surface Area (mm^2)	Villus Length (μm)	Depth of crypts (μM)
No Injection	10998.86 ± 305.72^{c}	154.70 ± 3.17^{d}	25.17 ± 0.92^{ab}
H_2O Injection	20515.14 ± 502.93^{a}	267.21 ± 4.30^{a}	26.35 ± 0.98^{a}
5% BCSE	13310.78 ± 3.79^{b}	193.07 ± 3.79^{c}	24.37 ± 0.94^{ab}
15% BCSE	20161.03 ± 4.02^{a}	250.78 ± 4.02^{b}	23.00 ± 0.78^{b}

Values are means ± SEM, $n = 5$/group. $^{a\text{-}d}$ Treatment groups not indicated by the same letter are different ($p < 0.05$) by *post hoc* Duncan test. BCSE: black corn soluble extract.

control groups (No Injection and H_2O Injection). Related to the cytokines, the IL1 was similar among all groups, while the pro-inflammatory IL6 was downregulated in the 5% and 15% BCSE ($p < 0.05$) compared to the H_2O Injection group.

3.6. Effect of black corn soluble extract on glycogen concentration and hepatic gene expression

The 5% BCSE and 15% BCSE treatment increased ($p < 0.05$) the hepatic glycogen concentration compared to the No Injection and H_20 Injection group. The pectoral glycogen concentration was not detectable in both control groups (No Injection and H_20 Injection); however, it was verified in both treatment groups with BCSE (5 and 15%) (Fig. 3).

Therefore, as the black corn soluble extract increased the pectoral and hepatic glycogen, we further investigated hepatic glucose and glycogen metabolism enzymes. The gene expression of the enzymes glucose-6 phosphatase (G6PD) and phosphofructokinase (PFK) did not differ ($p > 0.05$, Fig. 3) among all the treatment groups. Further, the gene expression of phosphoenolpyruvate carboxykinase (PCK1) was upregulated ($p < 0.05$) in the 15% BCSE compared to the No Injection group. However, there was no difference between the 5% BCSE or 15% BCSE and the H_2O Injection (Fig. 3).

3.7. Effect of black corn soluble extract on duodenal morphological parameters

The BCSE intra-amniotic administration promoted specific improvements on the small intestine morphological features. First, the intra-amniotic administration of 15% BCSE increased the villi surface area compared to the No Injection group ($p < 0.05$). Further, we observed that a higher concentration of BCSE (15%) promoted an increase of the villi surface area compared to a low concentration (5%) ($p < 0.05$). In the same way, the 15% BCSE increased the villus length ($p < 0.05$) compared to the No Injection and 5% BCSE. Regarding the depth of crypts, the 15% BCSE was similar to the No Injection group and was lower ($p < 0.05$) than the H_2O Injection group (Table 5).

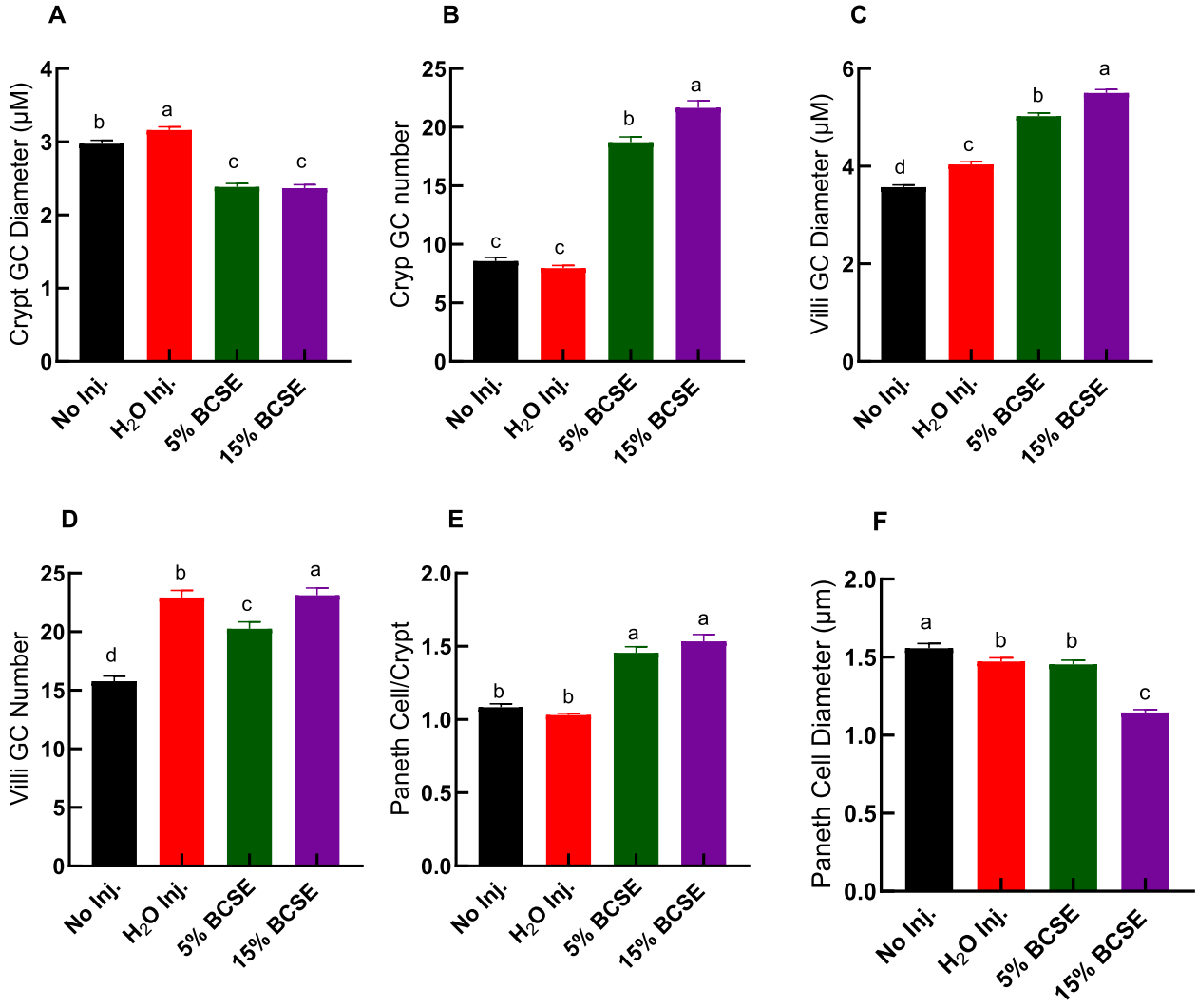

Fig. 4. Effect of black corn soluble extract on the goblet cells and Paneth cells. Values are means ± SEM, $n = 5$/group. $^{a\text{-}d}$ Treatment groups not indicated by the same letter are different ($p < 0.05$) by *post hoc* Duncan test. BCSE: black corn soluble extract.

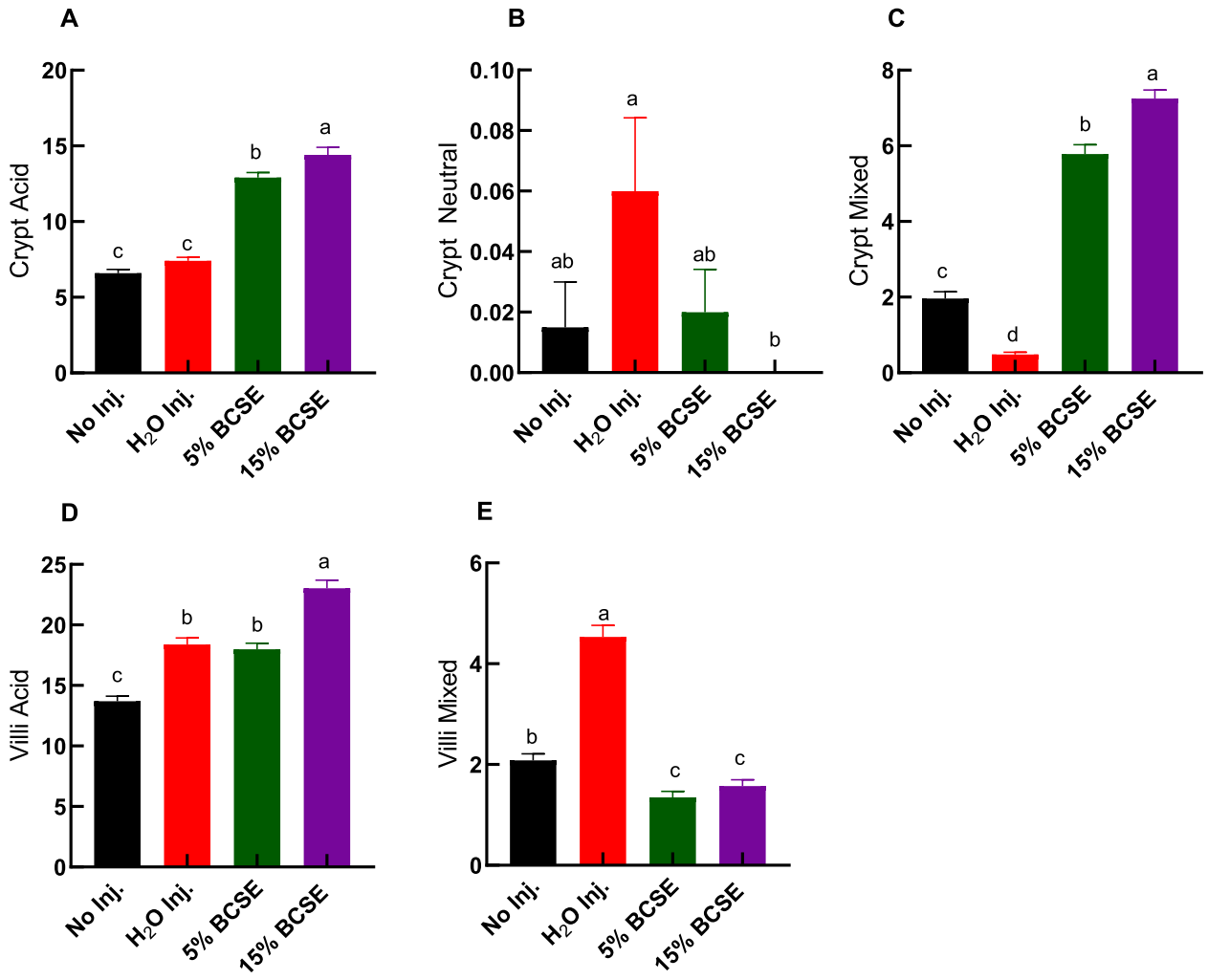

Fig. 5. Effect of black corn soluble extract on the acid, neutral and mixed goblet cells. Values are means ± SEM, $n = 5$/group. [a-d] Treatment groups not indicated by the same letter are different ($p < 0.05$) by *post hoc* Duncan test. BCSE: black corn soluble extract.

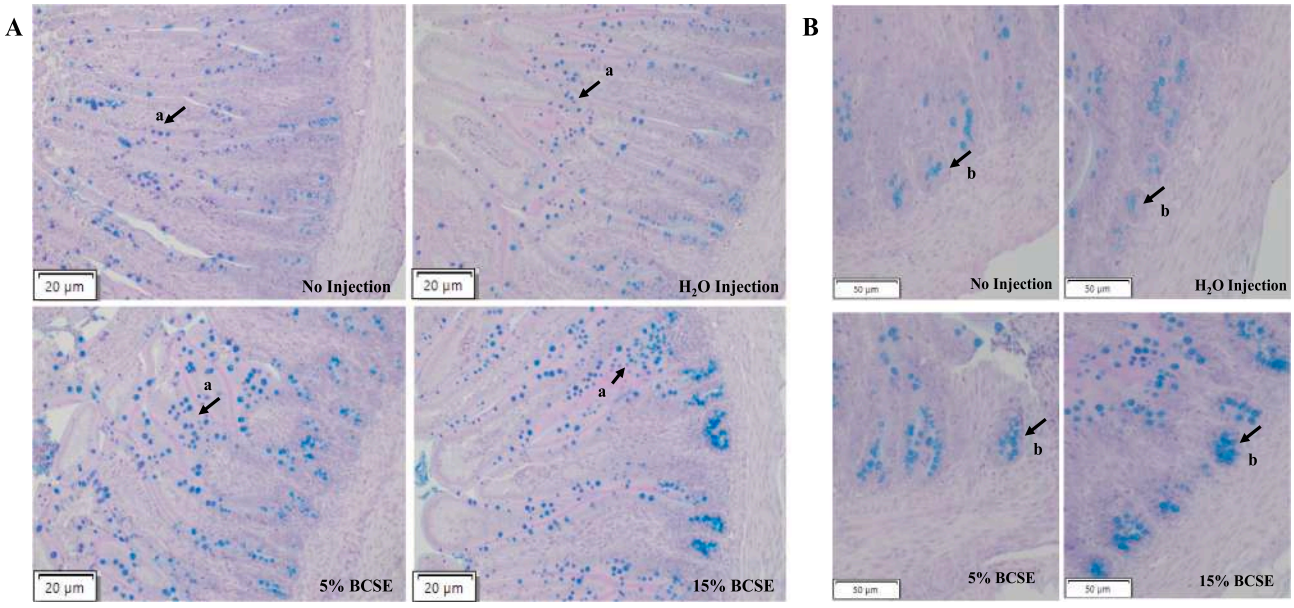

Fig. 6. Representative of the intestinal morphology. A: goblet cells on the villi for each treatment group; B: goblet cell on the crypt for each treatment group. Black arrows represent the increase of goblet cell at specif locations: (a): goblet cell on the villi; (b) goblet cell on the crypts.

In addition, the intra-amniotic administration of BCSE showed effects on the goblet cells (GC). In the crypt, the goblet cells diameter was lower ($p < 0.05$) in the 5% and 15% BCSE groups than in the H_2O Injection and No Injection groups. On the other hand, the number of crypt goblet cells where higher ($p < 0.05$) in both groups that had the BCSE (5 and 15%) intra-amniotic administration. Moreover, in the villi, the goblet cells diameter was higher ($p < 0.05$) following the 5% and 15% BCSE intra-amniotic administration compared to the No Injection and H_20 Injection. In the same way, the villi GC number showed an increase in the 5% and 15% BCSE groups ($p < 0.05$) compared to the No Injection group. In addition, the number of Paneth cells in the crypt was higher in the 5% and 15% BCSE groups than the No Injection and H_2O Injection. On the other hand, the Paneth cell diameter decreased in the 15% BCSE compared to the No Injection, H_2O Injection, and 5% BCSE (Figs. 4 and 6).

The types of goblet cells were classified as acid, neutral or mixed. In the crypt, the 5% and 15% of BCSE promoted an increase ($p < 0.05$) of acidic and mixed goblet cells compared to the No Injection and H_2O Injection groups. The neutral reduced ($p < 0.05$) in the 15% BCSE compared to the H_2O Injection. Further, in the villi, there was an increase ($p < 0.05$) of the acid goblet cell in the 15% BCSE compared to the No Injection and H_20 Injection, and in the 5% BCSE compared to the No Injection. On the other hand, the mixed goblet cell decreased ($p < 0.05$) in both BCSE treatments compared to the controls. No neutral cells were identified in the villi of all experimental groups (data not showed) (Fig. 5).

4. Discussion

In the present study, the intra-amniotic administration (*Gallus gallus*) of black corn soluble extract (BCSE), as a source of anthocyanin, demonstrated an anti-inflammatory effect that promoted a change in the microbiota bacterial abundance, improved biomarkers of the physical intestinal barrier and the mucus layer.

Colored maize has been a target of interest due to its natural pigments and its health effects (van Hung, 2014; Zhu, 2018). In the black corn used to elaborate the soluble extract of the current experiment, the total anthocyanin content was 85.65 mg/100 g, in which the major anthocyanidin was the cyanidin-3-glucoside (C3O) (30.40 mg/100 g). Anthocyanins have low bioavailability through the upper intestinal tract; thus, a significant amount reaches the colon intact and undergoes the gut microbiota metabolism. First, the colonic microbiota hydrolyses glycosides into aglycones, and then in a second phase, they are degraded into phenolic acids (Tian et al., 2018).

The BCSE intra-amniotic administration changed the intestinal microbiota composition and function by elevating specific bacteria genus density. The BCSE (5 and 15%) increased the *E. coli* abundance compared to the H_2O Injection group (Fig. 1). It is suggested that species in the *E. coli* genus are used as a substrate to anthocyanin metabolism, as authors showed that an anthocyanin extract promoted an enhancement of *E. coli*, thus suggesting that the anthocyanin was fermented by *E. coli* (Kuntz et al., 2016). In agreement with our results, an increase in the *E. coli* abundance was associated with the biotransformation of daidzein into its bioactive metabolites by the *E. coli* genus (Hartono et al., 2015), suggesting that species at the *E Coli* genus are involved in the intestinal metabolism of bioactive components. Furthermore, the 5% BCSE increased the *Clostridium* abundance compared to the No Injection group. This genus includes anaerobic species as the *Clostridium butyricum*, which improves the intestinal integrity by producing short-chain fatty acids (SCFA), mainly butyrate and acetate due fermentation (Stoeva et al., 2021). Therefore, the increase in *E. coli* and *Clostridium* abundance following the BCSE might be associated with species included in these genus, that are responsible to metabolize the anthocyanin into its phenolic acids producing SCFA.

In addition, the BCSE (5 and 15%) increased the glycogen levels (hepatic and pectoral). Thus, we further evaluated specific hepatic enzymes that are involved in glucose metabolism. However, the gene expression of G6PD, and PKF was not affected by the BCSE administration. Therefore, we suggest that the glycogen increase might be associated with SCFA production (Stoeva, et al., 2021), since the *Clostridium* abundance increased, which is a genus composed of butyrate-producing bacteria. Furthermore, the BCSE showed an effect in only one of the brush border functional proteins evaluated. The BCSE upregulated the SGLT1 gene expression, which might be explained as anthocyanin glycosides are absorbed through the SGLT1 transport in the small intestine (Fang, 2014).

Regarding the inflammatory biomarkers assessed in the duodenum, the BCSE (5% and 15%) downregulated the gene expression of NF-κB, IL6 and TNF-α. The transcriptional factor NF-κB is responsible for controlling physiological and pathological processes by inducing cytokine gene expression to control inflammatory and immune responses (Baker et al., 2011). The NF-κB complex stays in the cytosol and after stimulus is translocated into the nucleus to drive the expression of target genes as TNF-α, IL1β, IL6 and IL10 (Yu et al., 2020). In our experiment, the BCSE suppressed the inflammation by downregulating the NF-κB, decreasing expression of pro-inflammatory cytokines trigged by the NF-κB pathway. This might be associated to the cyanidin-3-glucoside be the major anthocyanidin in the black corn flour used for this experiment. Furthermore, the NF-κB signaling is associated with an impaired barrier function due to inflammation, leading to increase intestinal permeability and bacterial translocation (Yu et al., 2020). Thus, we further evaluated biomarkers involved in the intestinal barrier integrity.

To the best of our knowledge, this study is the first *in vivo* demonstration of BCSE ability to upregulate AMPK and CDX2 gene expression. AMPK is an energy regulator and regulates the strength of the epithelial barrier function through enhancing the assembly and stability of apical junctions via the phosphorylation of tight junction's proteins (M. J. Zhu et al., 2018; Rowart et al., 2018; Tsukita et al., 2019). However, in this study, the AMPK upregulation did not improve the occludin (OCLN) following the BCSE administration. Thus, to improve the OCLN a higher dose of anthocyanins might be needed to exert this effect. Therefore, in our study, the AMPK upregulation may be associated to NF-κB pathway inhibition. Further, the AMPK was associated to CDX2 upregulation in the BCSE group. CDX2 is an intestine-specific transcriptional factor that induces epithelial cell differentiation and regulates genes in the tight junction complex (Coskun et al., 2011). Purple potato extract enhanced tight junction assembly by AMPK activation and CDX2 protein content in a *in vitro* study (Sun et al., 2018). Furthermore, CDX2 controls intestinal inflammation as CDX2 expression and its affinity to bind to target genes are suppressed by TNF-α signaling (Coskun et al., 2014).

The BCSE improved morphological features on the duodenum. First, the villi surface area increased following the 15% BCSE administration, which might be due to anthocyanin fermentation and intestinal metabolism by commensal microorganisms (Kuntz et al., 2016). Further, we observed an increase in goblet cell (GC) number in the crypt, but with a reduction in its size (diameter) following BCSE (15%). We suggest that the BCSE promoted the differentiation of stem cells into GC in the crypt to improve mucus production if needed. However, as the GC size in the crypt decreased, this might suggest that mucin was not overproduced since the organism was not challenging any microbial inflammation. The GC is composed mainly of mucins, which promote a gel-forming mucus layer to avoid the adhesion and invasion of pathogenic bacteria into the intestinal epithelium (Duangnumsawang et al., 2021). The mucin production on the crypt is more preserved than in the villi, as it is responsible for providing additional protection in gut inflammation (Schneider et al., 2018). On the other hand, on the villi the number but also the size of GC increased following the 15% BCSE administration. A higher mucin production in the villi compared to the crypt is associated with physiological action to promote luminal motility and to protect the epithelial surface from chemical and bacterial components (Schneider et al., 2018).

In the current study, the Paneth cells number increased in the crypt

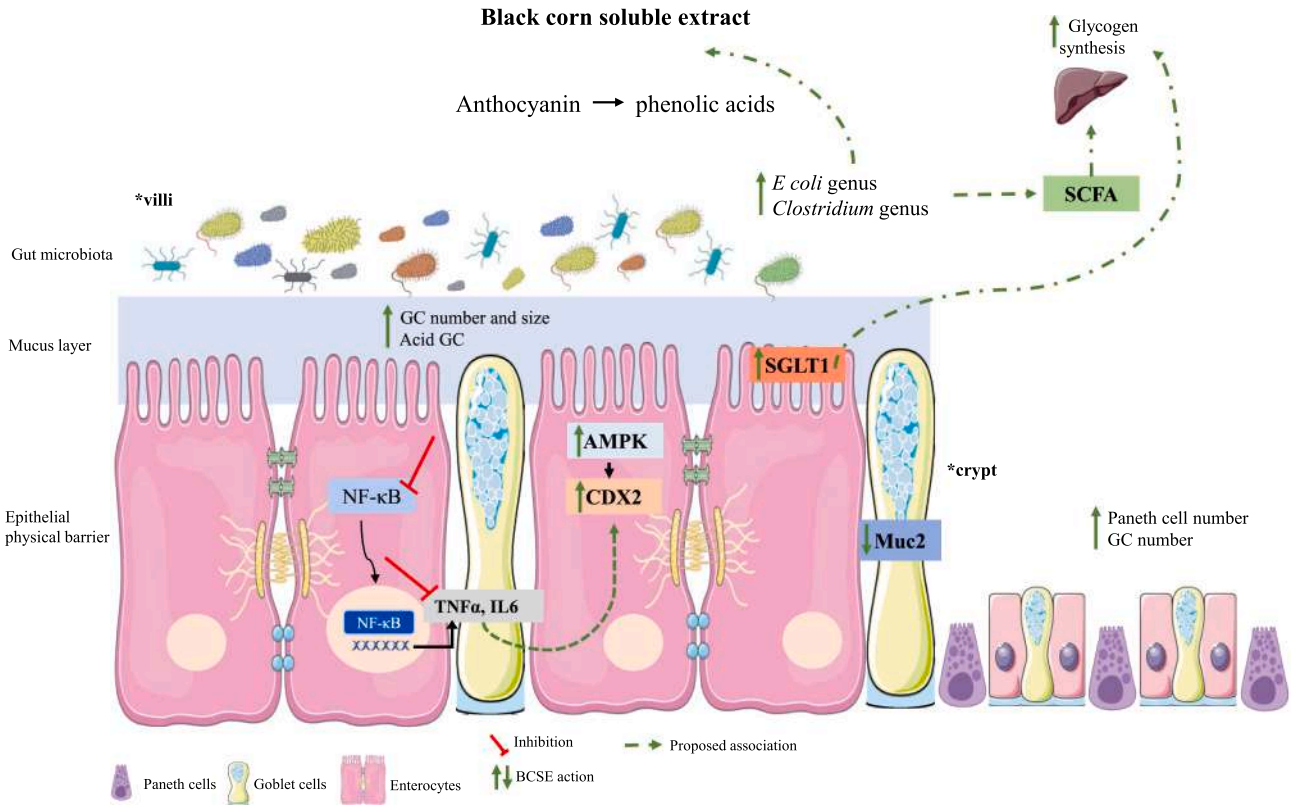

Fig. 7. Proposed mechanisms of black corn soluble extract to improve intestinal integrity. SCFA: short-chain fatty acids; NF-κB: nuclear factor kappa beta; TNF-α: tumor necrosis factor alpha; AMPK: adenosine monophosphate-activated protein kinase; CDX2: caudal-type homeobox 2; SGLT1: sodium-glucose transporter 1; MUC2: mucin 2.

and a reduced in its cell size. Paneth cells secrete antimicrobial peptides as α-defensin, Reg3 and lysozyme into the crypt lumen, after stimuli as pathogenic exposure (Gassler, 2017). Similar results were verified after the intra-amniotic administration of *C. sativus* flower as a source of flavonoids (Agarwal et al., 2022), therefore, we suggest that phenolics in the 5% BCSE improved the Paneth cell development without affecting this cell's size. This indicates that the antimicrobial peptides secreted by Paneth cells were not produced since there were no stimuli such as inflammation or pathogenic bacteria. Moreover, the 15% BCSE increased the acid GC on the crypt and the villi. Acid mucin creates a luminal acid pH, influencing the microbiota composition since pathogenic bacteria are less likely to survive in an acidic environment (Witten et al., 2018). Further, MUC2 is one of the major components of mucins (Tarabova et al., 2016), and the BCSE administration downregulated the MUC2 in this study. The NF-κB has been described as a target of MUC2 expression so that the TNF-α promotes the NF-κB translocation, thus inducing the MUC2 expression (Iwashita et al., 2003; Paone & Cani, 2020).

Finally, the intra-amniotic administration of black corn soluble extract in the *Gallus gallus* model promoted an increase in *E. coli* and *Clostridium* abundance, which were associated with butyrate-producing bacteria and the intestinal metabolism of anthocyanin by breaking it into phenolic acids. The BCSE promoted an anti-inflammatory effect via down-regulating the NF-κB, TNF-α and IL6 on the duodenum, which improved biomarkers on the intestinal physical barrier as AMPK and CDX2. The BCSE increased the glycogen synthesis associated with the transporter SGLT1 in the small intestine. The BCSE improve the morphological structure of the duodenum, by increasing the number of Paneth cell and goblet cell populations in the crypt, and the number and size of villi goblet cell, with specific increase in acidic goblet cell population in the crypt and villi. Thus, improving the mucus layer to act as a barrier against pathogens and pathogenic components (Fig. 7).

5. Conclusion

The intra-amniotic administration of black corn soluble extract as a source of anthocyanins promoted positive function on the intestinal barrier. The BCSE showed anti-inflammatory properties, promoted changes in the relative abundance of gut bacteria, improved the mucus layer and upregulated biomarkers of the physical epithelial barrier. Therefore, the black corn can be a focus of further research and be stimulated as a strategy to improve the diet composition as a additional source of anthocyanins.

CRediT authorship contribution statement

Thaisa Agrizzi Verediano: Data curation, Formal analysis, Investigation, Methodology, Writing – original draft. **Hércia Stampini Duarte Martino:** Investigation, Writing – original draft, Supervision, Resources. **Nikolai Kolba:** Data curation, Formal analysis, Investigation, Methodology. **Yimin Fu:** Data curation, Formal analysis, Writing – original draft. **Maria Cristina Dias Paes:** Supervision, Resources. **Elad Tako:** Data curation, Formal analysis, Investigation, Writing – original draft, Supervision, Resources.

Declaration of Competing Interest

The authors declare that they have no known competing financial interests or personal relationships that could have appeared to influence the work reported in this paper.

Acknowledgments

The authors would like to thank the Coordination for the Improvement of Higher Educational Personnel (CAPES), Brazil, for TAV doctor's

scholarship support in the Capes-Print Program (process number 88887.569929/2020-00), and the National Council of Technological and Scientific Development (CNPq, Brazil) for Research Productivity grants, and the Embrapa (Brazil) for providing the black corn and the anthocyanin profile.

References

Agarwal, N., Kolba, N., Jung, Y., Cheng, J., & Tako, E. (2022). Saffron (Crocus sativus L.) Flower Water Extract Disrupts the Cecal Microbiome, Brush Border Membrane Functionality, and Morphology In Vivo (Gallus gallus). *Nutrients, 14*(1), 220. https://doi.org/10.3390/nu14010220

AOAC International. (2012). *Official Methods of Analysis* (19th ed.). AOAC International.

Azzini, E., Giacometti, J., & Russo, G. L. (2017). Antiobesity Effects of Anthocyanins in Preclinical and Clinical Studies. *Oxidative Medicine and Cellular Longevity*, *2017*(ii), 1–11. https://doi.org/10.1155/2017/2740364.

Baker, R. G., Hayden, M. S., & Ghosh, S. (2011). NF- kB, Inflammation, and Metabolic Disease. *Cell Metabolism, 13*, 11–22. https://doi.org/10.1016/j.cmet.2010.12.008

Bendokas, V., Stanys, V., Mažeikienė, I., Trumbeckaite, S., Baniene, R., & Liobikas, J. (2020). Anthocyanins: From the field to the antioxidants in the body. *Antioxidants, 9*(9), 1–16. https://doi.org/10.3390/antiox9090819

Bhaswant, M., Shafie, S. R., Mathai, M. L., Mouatt, P., & Brown, L. (2017). Anthocyanins in chokeberry and purple maize attenuate diet-induced metabolic syndrome in rats. *Nutrition, 41*, 24–31.

Carboni, J., Reed, S., Kolba, N., Eshel, A., Koren, O., & Tako, E. (2020). Alterations in the intestinal morphology, gut microbiota, and trace mineral status following intra-amniotic administration (Gallus gallus) of teff (eragrostis tef) seed extracts. *Nutrients, 12*(3020), 1–18. https://doi.org/10.3390/nu12103020

Cremonini, E., Daveri, E., Mastaloudis, A., Adamo, A. M., Mills, D., Kalanetra, K., … Oteiza, P. I. (2019). Anthocyanins protect the gastrointestinal tract from high fat diet-induced alterations in redox signaling, barrier integrity and dysbiosis. *Redox Biology, 26*(June), Article 101269. https://doi.org/10.1016/j.redox.2019.101269

Coskun, M., Olsen, A. K., Bzorek, M., Holck, S., Engel, U. H., Nielsen, O. H., & Troelsen, J. T. (2014). Involvement of CDX2 in the cross talk between TNF-α and Wnt signaling pathway in the colon cancer cell line Caco-2. *Carcinogenesis, 35*(5), 1185–1192. https://doi.org/10.1093/carcin/bgu037

Coskun, M., Troelsen, J. T., & Nielsen, O. H. (2011). The role of CDX2 in intestinal homeostasis and inflammation. In *Biochimica et Biophysica Acta - Molecular Basis of Disease* (Vol. 1812, Issue 3, pp. 283–289). https://doi.org/10.1016/j.bbadis.2010.11.008.

da Silva, B. P., Kolba, N., Martino, H. S. D., Hart, J., & Tako, E. (2019). Soluble extracts from chia seed (Salvia hispanica L.) affect brush border membrane functionality, morphology and intestinal bacterial populations in vivo (Gallus gallus). *Nutrients, 11*(2457), 1–17. https://doi.org/10.3390/nu11102457

de Sousa Moraes, L. F., Sun, X., Peluzio, M. do C. G., & Zhu, M. J. (2019). Anthocyanins/anthocyanidins and colorectal cancer: What is behind the scenes? *Critical Reviews in Food Science and Nutrition*, *59*(1), 59–71. https://doi.org/10.1080/10408398.2017.1357533.

Dias, D. M., Kolba, N., Hart, J. J., Ma, M., Sha, S. T., Lakshmanan, N., … Tako, E. (2019). Soluble extracts from carioca beans (Phaseolus vulgaris L.) affect the gut microbiota and iron related brush border membrane protein expression in vivo (Gallus gallus). *Food Research International, 123*, 172–180. https://doi.org/10.1016/j.foodres.2019.04.060

Dreiling, C. E., Brown, D. E., Casale, L., & Kelly, L. (1987). Muscle Glycogen: Comparison of Iodine Binding and Enzyme Digestion Assays and Application to Meat Samples. *Meat Science, 20*(t987), 167–177.

Duangnumsawang, Y., Zentek, J., & Goodarzi Boroojeni, F. (2021). Development and Functional Properties of Intestinal Mucus Layer in Poultry. In *Frontiers in Immunology* (Vol. 12, pp. 1–18). Frontiers Media S.A. https://doi.org/10.3389/fimmu.2021.745849.

Fang, J. (2014). Bioavailability of anthocyanins. *Drug Metabolism Reviews, 46*(4), 508–520. https://doi.org/10.3109/03602532.2014.978080

Faria, A., Fernandes, I., Norberto, S., Mateus, N., & Calhau, C. (2014). Interplay between anthocyanins and gut microbiota. *Journal of Agricultural and Food Chemistry, 62*(29), 6898–6902. https://doi.org/10.1021/jf501808a

Fernández, J., García, L., Monte, J., Villar, C. J., & Lombó, F. (2018). Functional anthocyanin-rich sausages diminish colorectal cancer in an animal model and reduce pro-inflammatory bacteria in the intestinal microbiota. *Genes, 9*(3), 1–17. https://doi.org/10.3390/genes9030133

Gassler, N. (2017). Paneth cells in intestinal physiology and pathophysiology. *World Journal of Gastrointestinal Pathophysiology, 8*(4), 150–160. https://doi.org/10.4291/wjgp.v8.i4.150

Gomes, M. J. C., Kolba, N., Agarwal, N., Kim, D., Eshel, A., Koren, O., & Tako, E. (2021). Modifications in the intestinal functionality, morphology and microbiome following intra-amniotic administration (Gallus gallus) of grape (vitis vinifera) stilbenes (resveratrol and pterostilbene). *Nutrients, 13*(3247), 1–19. https://doi.org/10.3390/nu13093247

Guo, H., Ling, W., Wang, Q., Liu, C., Hu, Y., Xia, M., … Xia, X. (2007). Effect of anthocyanin-rich extract from black rice (Oryza sativa L. indica) on hyperlipidemia and insulin resistance in fructose-fed rats. *Plant Foods for Human Nutrition, 62*(1), 1–6. https://doi.org/10.1007/s11130-006-0031-7

Harakotr, B., Suriharn, B., Tangwongchai, R., Scott, M. P., & Lertrat, K. (2014). Anthocyanins and antioxidant activity in coloured waxy corn at different maturation stages. *Journal of Functional Foods, 9*(1), 109–118. https://doi.org/10.1016/j.jff.2014.04.012

Hartono, K., Reed, S., Ankrah, N. A., Glahn, R. P., & Tako, E. (2015a). Alterations in gut microflora populations and brush border functionality following intra-amniotic daidzein administration. *RSC Advances, 5*(9), 6407–6412. https://doi.org/10.1039/c4ra10962g

Hartono, K., Reed, S., Ankrah, N. A., Glahn, R. P., & Tako, E. (2015b). Alterations in gut microflora populations and brushborder functionality following intra-amnioticdaidzein administration. *RSC Advances, 5*, 6407–6412. https://doi.org/10.1039/C4RA10962G

Hou, T., Kolba, N., Glahn, R., & Tako, E. (2017). Intra-Amniotic Administration (Gallus gallus) of Cicer arietinum and Lens culinaris Prebiotics Extracts and Duck Egg White Peptides Affects Calcium Status and Intestinal Functionality. *Nutrients, 9*(7), 785. https://doi.org/10.3390/nu9070785

Hou, T., & Tako, E. (2018). The in Ovo feeding administration (Gallus gallus)—An emerging in vivo approach to assess bioactive compounds with potential nutritional benefits. *Nutrients, 10*(4), 1–17. https://doi.org/10.3390/nu10040418

Hribar, U., & Ulrih, P. (2014). The Metabolism of Anthocyanins. *Current Drug Metabolism, 15*, 3–13.

Iwashita, J., Sato, Y., Sugaya, H., Takahashi, N., Sasaki, H., & Abe, T. (2003). mRNA of MUC2 is stimulated by IL-4, IL-13 or TNF-α through a mitogen-activated protein kinase pathway in human colon cancer cells. *Immunology and Cell Biology, 81*(4), 275–282. https://doi.org/10.1046/j.1440-1711.2003.t01-1-01163.x

Jamar, G., Estadella, D., & Pisani, L. P. (2017). Contribution of anthocyanin-rich foods in obesity control through gut microbiota interactions. *BioFactors, 43*(4), 507–516. https://doi.org/10.1002/biof.1365

Jurgoński, A., Juśkiewicz, J., & Zduńczyk, Z. (2013). An anthocyanin-rich extract from Kamchatka honeysuckle increases enzymatic activity within the gut and ameliorates abnormal lipid and glucose metabolism in rats. *Nutrition, 29*(6), 898–902. https://doi.org/10.1016/j.nut.2012.11.006

Kuntz, S., Kunz, C., Domann, E., Würdemann, N., Unger, F., Römpp, A., & Rudloff, S. (2016). Inhibition of low-grade inflammation by anthocyanins after microbial fermentation in vitro. *Nutrients, 8*(411), 1–19. https://doi.org/10.3390/nu8070411

Lee, Y.-M., Yoon, Y., Park, H.-M., Song, S., & Yeum, K.-J. (2017). Dietary Anthocyanins against Obesity and Inflammation. *Nutrients, 9*(1089), 1–15. https://doi.org/10.3390/nu9101089

Martino, H. S. D., Kolba, N., & Tako, E. (2020). Yacon (Smallanthus sonchifolius) flour soluble extract improve intestinal bacterial populations, brush border membrane functionality and morphology in vivo (Gallus gallus). *Food Research International, 137*(109705). https://doi.org/10.1016/j.foodres.2020.109705

Paone, P., & Cani, P. D. (2020). Mucus barrier, mucins and gut microbiota: The expected slimy partners? In *Gut* (Vol. 69, Issue 12, pp. 2232–2243). BMJ Publishing Group. https://doi.org/10.1136/gutjnl-2020-322260.

Paulsmeyer, M., Chatham, L., Becker, T., West, M., West, L., & Juvik, J. (2017). Survey of Anthocyanin Composition and Concentration in Diverse Maize Germplasms. *Journal of Agricultural and Food Chemistry, 65*(21), 4341–4350. https://doi.org/10.1021/acs.jafc.7b00771

Ranilla, L. G., Christopher, A., Sarkar, D., Shetty, K., Chirinos, R., & Campos, D. (2017). Phenolic Composition and Evaluation of the Antimicrobial Activity of Free and Bound Phenolic Fractions from a Peruvian Purple Corn (Zea mays L.) Accession. *Journal of Food Science*, 1–9. https://doi.org/10.1111/1750-3841.13973

Rowart, P., Wu, J., Caplan, M. J., & Jouret, F. (2018). Implications of AMPK in the formation of epithelial tight junctions. *International Journal of Molecular Sciences, 19*(7). https://doi.org/10.3390/ijms19072040

Różańska, D., & Regulska-Ilow, B. (2018). The significance of anthocyanins in the prevention and treatment of type 2 diabetes. *Adv Clin Exp Med, 27*(1), 135–142. https://doi.org/10.17219/acem/64983.

Schneider, H., Pelaseyed, T., Svensson, F., & Johansson, M. E. V. (2018). Study of mucin turnover in the small intestine by in vivo labeling. *Scientific Reports, 5760*(1), 1–8. https://doi.org/10.1038/s41598-018-24148-x

Stoeva, M. K., Garcia-So, J., Justice, N., Myers, J., Tyagi, S., Nemchek, M., McMurdie, P. J., Kolterman, O., & Eid, J. (2021). Butyrate-producing human gut symbiont, Clostridium butyricum, and its role in health and disease. In *Gut Microbes* (Vol. 13, Issue 1, pp. 1–28). Bellwether Publishing, Ltd. https://doi.org/10.1080/19490976.2021.1907272.

Sui, X., Zhang, Y., Jiang, L., & Zhou, W. (2019). Anthocyanins in Food. *Encyclopedia of Food Chemistry, 2*, 10–17.

Sun, X., Du, M., Navarre, D. A., & Zhu, M. J. (2018). Purple Potato Extract Promotes Intestinal Epithelial Differentiation and Barrier Function by Activating AMP-Activated Protein Kinase. *Molecular Nutrition and Food Research, 62*(4). https://doi.org/10.1002/mnfr.201700536

Tako, E., Glahn, R. P., Knez, M., & Stangoulis, J. C. (2014). The effect of wheat prebiotics on the gut bacterial population and iron status of iron deficient broiler chickens. *Nutrition Journal, 13*(58), 1–10. https://doi.org/10.1186/1475-2891-13-58

Tako, E., Glahn, R. P., Welch, R. M., Lei, X., Yasuda, K., & Miller, D. D. (2008). Dietary inulin affects the expression of intestinal enterocyte iron transporters, receptors and storage protein and alters the microbiota in the pig intestine. *British Journal of Nutrition, 99*(3), 472–480. https://doi.org/10.1017/S0007114507825128

Tarabova, L., Makova, Z., Piesova, E., Szaboova, R., & Faixova, Z. (2016). Intestinal Mucus Layer and Mucins (A Review). *Folia Veterinaria, 60*(1), 21–25. https://doi.org/10.1515/fv-2016-0003

Tian, L., Tan, Y., Chen, G., Wang, G., Sun, J., Ou, S., … Bai, W. (2018). Metabolism of anthocyanins and consequent effects on the gut microbiota. *Critical Reviews in Food Science and Nutrition, 59*(6), 982–991. https://doi.org/10.1080/10408398.2018.1533517

Tong, T., Niu, Y. H., Yue, Y., Wu, S. chan, & Ding, H. (2017). Beneficial effects of anthocyanins from red cabbage (Brassica oleracea L. var. capitata L.) administration to prevent irinotecan-induced mucositis. *Journal of Functional Foods*, *32*, 9–17. https://doi.org/10.1016/j.jff.2017.01.051.

Tsukita, K., Yano, T., Tamura, A., & Tsukita, S. (2019). Reciprocal association between the apical junctional complex and AMPK: A promising therapeutic target for epithelial/endothelial barrier function? In *International Journal of Molecular Sciences* (Vol. 20, Issue 23). MDPI AG. https://doi.org/10.3390/ijms20236012.

van Hung, P. (2014). Phenolic Compounds of Cereals and Their Antioxidant Capacity. *Critical Reviews in Food Science and Nutrition, 56*(1), 25–35. https://doi.org/10.1080/10408398.2012.708909

Vendrame, S., & Klimis-Zacas, D. (2015). Anti-inflammatory effect of anthocyanins via modulation of nuclear factor- kB and mitogen-activated protein kinase signaling cascades. *Nutrition Reviews, 73*(6), 348–358. https://doi.org/10.1093/nutrit/nuu066

Verediano, T. A., Stampini Duarte Martino, H., Dias Paes, M. C., & Tako, E. (2021). Effects of anthocyanin on intestinal health: A systematic review. In *Nutrients* (Vol. 13, Issue 1331, pp. 1–20). MDPI AG. https://doi.org/10.3390/nu13041331.

Wang, X., Kolba, N., Liang, J., & Tako, E. (2019). Alterations in gut microflora populations and brush border functionality following intra-amniotic administration (Gallus gallus) of wheat bran prebiotic extracts. *Food and Function, 10*(8), 4834–4843. https://doi.org/10.1039/c9fo00836e

Witten, J., Samad, T., & Ribbeck, K. (2018). Selective permeability of mucus barriers. *Current Opinion in Biotechnology, 52*, 124–133. https://doi.org/10.1016/j.copbio.2018.03.010

Yang, Z., & Zhai, W. (2010). Identification and antioxidant activity of anthocyanins extracted from the seed and cob of purple corn (Zea mays L.). *Innovative Food Science and Emerging Technologies, 11*(1), 169–176. https://doi.org/10.1016/j.ifset.2009.08.012

Yegani, M., & Korver, D. R. (2008). Factors affecting intestinal health in poultry. In *Poultry Science* (Vol. 87, Issue 10, pp. 2052–2063). Poultry Science Association. https://doi.org/10.3382/ps.2008-00091.

Yu, H., Lin, L., Zhang, Z., Zhang, H., & Hu, H. (2020). Targeting NF-κB pathway for the therapy of diseases: mechanism and clinical study. In *Signal Transduction and Targeted Therapy* (Vol. 5, Issue 1). Springer Nature. https://doi.org/10.1038/s41392-020-00312-6.

Zhang, Q., de Mejia, E. G., Luna-Vital, D., Tao, T., Chandrasekaran, S., Chatham, L., … Kumar, D. (2019). Relationship of phenolic composition of selected purple maize (Zea mays L.) genotypes with their anti-inflammatory, anti-adipogenic and anti-diabetic potential. *Food Chemistry, 289*, 739–750. https://doi.org/10.1016/j.foodchem.2019.03.116

Zhu, F. (2018). Anthocyanins in cereals: Composition and health effects. *Food Research International, 109*, 232–249.

Zhu, M. J., Sun, X., & Du, M. (2018). AMPK in regulation of apical junctions and barrier function of intestinal epithelium. In *Tissue Barriers* (Vol. 6, Issue 2, pp. 1–13). Taylor and Francis Inc. https://doi.org/10.1080/21688370.2018.1487249.